ROYAL SOCIETY
OF CHEMISTRY

PAPER

Check for updates

Reduction of Au^{3+} to distinctive Au-based materials by amphiphilic sodium dodecylbenzenesulfonate†

Yao-Tsung Hsu,‡[ab] Hung-Fei Chen,‡[b] Wei-Jhih Lin,[c] Jungshan Chang*[a] and Fu-Der Mai [ID] *[ab]

Based on their morphologies or states, Au-based materials will be operative under a specific aqueous or organic phase. Reduction of Au^{3+} by amphiphilic sodium dodecylbenzenesulfonate is proposed to improve the phase challenge *via* an amphiphilic nature. Moreover, the green approach is expected to be suitable to prepare myriad Au-based materials which can be applied with a limited phase problem.

In recent years, research on Au-based materials, especially Au nanoparticles (AuNPs), Au nanoclusters (AuNCs) and composites of Au, has been widely studied.[1–4] These materials can be applied in a variety of fields including catalysis, sensing, biomedicine, *etc.*[5–10] States or morphologies, not surprisingly, will affect the resulting functionalities.[1–10] For instance, larger-sized AuNPs and the bulk gold supported on the metal oxides are usually catalytically inert, while small AuNCs (1–5 nm) show interesting catalytic activity toward the oxidation reactions, for defects in metal oxides can trap small AuNCs more efficiently.[11] Due to the variety of Au-based materials, efficacious routes for the extensive set of Au-based materials syntheses, such as size-controlled synthesis of AuNPs, have been studied by numerous scientists.[12–14] On the other hand, Au$^+$ complexes and AuNCs can be prepared using coordination chemistry. Organic ligands, such as triphenylphosphine (P(Ph)$_3$), are often used in order to form stable Au$^+$ complex.[15,16] However, organic solvents are required to dissolve these organic ligands. This may be a drawback in some fields, like biomedical applications, in which aqueous phase chemicals are preferred.[5,9,10,17,18]

Here, we propose a versatile colloidal reduction of Au^{3+} to resolve the phase challenge. In colloidal solution that contains amphiphilic colloids like surfactant molecules, these organic compounds such as ligands can disperse homogeneously in aqueous phase. Furthermore, the colloidal reduction of Au^{3+} can produce various categories of Au-based materials including size-controlled AuNPs, AuNCs, and AuNPs/graphene composite

ᵃGraduate Institute of Medical Sciences, College of Medicine, Taipei Medical University, Taipei 11031, Taiwan. E-mail: js.chang@tmu.edu.tw; fordmai@tmu.edu.tw

ᵇDepartment of Biochemistry and Molecular Cell Biology, School of Medicine, College of Medicine, Taipei Medical University, Taipei 11031, Taiwan

ᶜDepartment of Forensic Science, Central Police University, No. 56, Shujen Road, Taoyuan City 33304, Taiwan

† Electronic supplementary information (ESI) available. See DOI: 10.1039/d0ra07066a

‡ These authors contributed equally to this work.

via colloidal chemistry which is powerful in numerous synthetic routes.[19–23] Moreover, the proposed approach is a simple, low-cost, free of hazardous chemicals, and scalable one-pot synthesis.

Several reagents with sulphur-based functional groups were proved to be effective in reducing Au^{3+}.[14,24,25] In light of these researches, as a result, the sulfonate group of amphiphilic colloids which is often seen in surfactant molecules is used as the reacting site for the reduction of Au^{3+}.

During experiments, HAuCl$_4$ was added into sodium dodecylbenzenesulfonate (SDBS) solution. Besides its sulphur-based functional group that can reduce Au^{3+} effectively, SDBS is a widely used surfactant that can form micelles. Therefore, the reduction of Au^{3+} can be regulated using colloidal chemistry. In colloidal chemistry, critical micelle concentration (CMC) is an important factor.[26] In brief, if the concentration of the surfactant is above CMC, micelles will form, and the properties of the colloidal solution will change significantly. For nanoparticle synthesis, micelles can define the size of the resulting materials, thus, AuNPs, instead of bulk gold, can be produced more effectively.[20]

Generally, the formation of AuNPs takes three steps: reduction, nucleation, and growth.[27,28] Acknowledging the mechanism, we hypothesize that if the concentration of SDBS is above CMC, SDBS can reduce Au^{3+} well, stabilize initial nucleus using its amphiphilic nature and assist the growth process *via* micelle–micelle coalescence.

In classical nucleation, the critical radius (r_{cri}), the minimum size for a stable nanoparticle in the solution, depends on the surface tension (γ) and the degree of supersaturation ($\ln(C/C_0)$).[27,28] More specifically:

$$r_{\mathrm{cri}} \propto \frac{\gamma}{\ln\left(\dfrac{C}{C_0}\right)}$$

Therefore, the amphiphilic nature of SDBS is beneficial for nanoparticle synthesis, for it can reduce surface tension

remarkably once the concentration is above CMC. To further regulate the size of AuNPs, the degree of supersaturation becomes the key factor because the surface tension does not change significantly once the concentration is above CMC. The degree of supersaturation is highly related to chemical kinetics. A fast reaction usually results in a larger degree of supersaturation, and smaller nanoparticles would be synthesized.[27] Since the reaction rate is associated with the concentration of the reactant, a higher concentration of SDBS will have smaller AuNPs synthesized.

Furthermore, in the growth process, mass transfer plays an important role. The mass transfer is governed by Fick's law:[28]

$$j = -D\frac{\mathrm{d}C}{\mathrm{d}x}$$

where J is the total flux, D is the diffusivity, and $\mathrm{d}C/\mathrm{d}x$ is the concentration gradient. The amount of micelle would affect the diffusivity since micelles occupy some spaces.[29,30] For a higher concentration, the diffusivity is smaller due to the additional micelles, as a result, two nucleus are harder to collide and a large size of AuNPs would not grow. Based on the mechanism, a small size AuNPs will form under a high concentration of SDBS since (i) the fast reaction results in a small critical radius; (ii) additional micelles cause a smaller diffusivity and AuNPs will not grow too large. By controlling chemical kinetics and colloidal chemistry, different sizes of AuNPs can be synthesized. In experiments, 0.03, 0.1, 0.15, 0.2, 1.0 wt% SDBS are used as the demonstrations of size-controlled synthesis. For 0.03 wt% SDBS group, the concentration is below CMC (see ESI Fig. S1†).[31] Although Au^{3+} would partially nucleated and AuNPs with a 37.87 nm average diameter (Standard deviation (SD) 7.88 nm) can be synthesized based on Transmission electron microscopy (TEM) (Fig. 1a), other ions would become bulk gold with unpolished dark brown colour because of the lack of micelles. On the other hand, the concentration is just above CMC for 0.1 wt% SDBS group, thus, AuNPs can be synthesized effectively with a violet colour and with a 28.35 nm average diameter (SD 7.18 nm) characterized using TEM (Fig. 1b). In addition, the 0.15 and 0.2 wt% SDBS groups possess violet red and red colour, respectively. The average diameter is 16.99 nm for 0.15 wt% SDBS group (SD 4.43 nm) and 15.04 nm for 0.2 wt% SDBS group (SD 3.33 nm) (Fig. 1c and d). To synthesize sub-10 nanometer AuNPs, an even higher concentration, the 1.0 wt% SDBS group, was carried out and the average diameter is 9.23 nm (SD 1.63 nm) (Fig. 1e). The microscopic results indicate that the diameter of AuNPs does decrease as the concentration of SDBS increases. Additionally, the obvious wavelength shifts and colour changes of AuNPs solutions can be observed using UV-visible spectra (Fig. 1f) and the optical picture (Fig. 1g). The statistic colour changes of AuNPs solutions can be observed using UV-visible spectra (Fig. 1f) and the optical picture (Fig. 1g). The statistic results are shown in ESI Fig. S2.†

The optimal condition is summarized in Table S1.† At the starting point, we focus on a versatile and green reduction process to synthesize Au-based materials. The optimal condition has to produce more categories of Au-based materials (versatile) and reduce energy input as well as time consumption
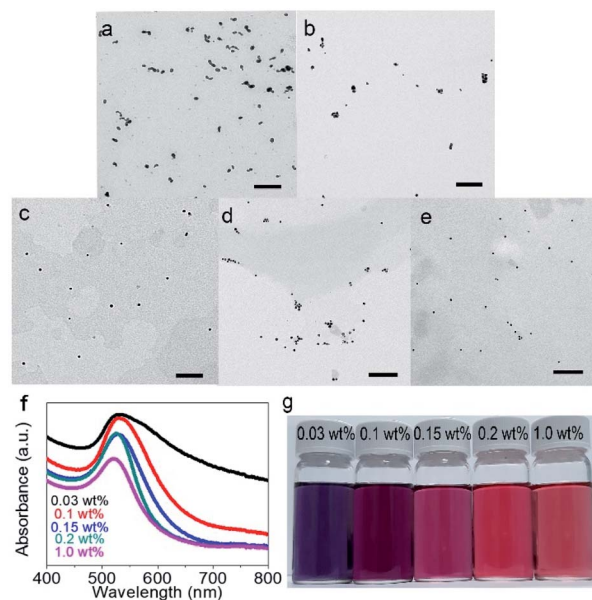

Fig. 1 Characterizations of size-controlled AuNPs. The scale bars in TEM are 200 nm. (a) TEM image of 0.03 wt% SDBS group. (b) TEM image of 0.1 wt% SDBS group. (c) TEM image of 0.15 wt% SDBS group. (d) TEM image of 0.2 wt% SDBS group. (e) TEM image of 1.0 wt% SDBS group. (f) UV-visible spectra show obvious wavelength shifts of AuNPs solutions. (g) Apparent colour changes can be observed by the optical picture.

(green). The optimal condition for reduction is under 90 °C, 20 minute reaction period, and 0.086 mM $HAuCl_4$, for size-controllable AuNPs can be synthesized fast. However, if the temperature is lower (60 °C), size-controllable synthesis is obviously poor according to the colours (Fig. S3a†). For an even lower temperature (30 °C), it takes 24 hours to synthesize AuNPs. Size-controllable synthesis, still, is poor (Fig. S3b†). Therefore, 90 °C is required to produce size-controllable AuNPs with a good efficiency. On the other hand, the concentration of precursors ($HAuCl_4$) cannot be too high since bulk gold rather than a nano-scale material would form (Fig. S3c†). This is because additional precursors make resultant products aggregate severely.

Besides AuNPs, AuNCs can be synthesized with coordination chemistry. With the presence of amphiphilic colloids, organic ligands can disperse homogeneously and coordination can occur under aqueous phase. In other words, there is no organic solvent. In experiments, $P(Ph)_3$ (10 equiv. with respect to $HAuCl_4$) is added to a $HAuCl_4$/SDBS solution. Instead of turning into colourful AuNPs, the colloidal solution becomes transparent, suggesting the formation Au^+ complex. With the protection of the ligands, Au^+ complex can be further reduced to small AuNCs rather than AuNPs by $NaBH_4$. The synthesis result is characterized by TEM (Fig. 2a) and the statistic result indicates the average diameter of AuNCs is 0.51 nm with a 0.15 nm SD (see ESI Fig. S4†). In addition, UV-visible spectrum of AuNCs contains a 470 nm absorption which does not appear in that of AuNPs (Fig. 2b).

To further demonstrate the advantage of colloidal reduction of Au^{3+}, we synthesized AuNPs/graphene composite by a simple
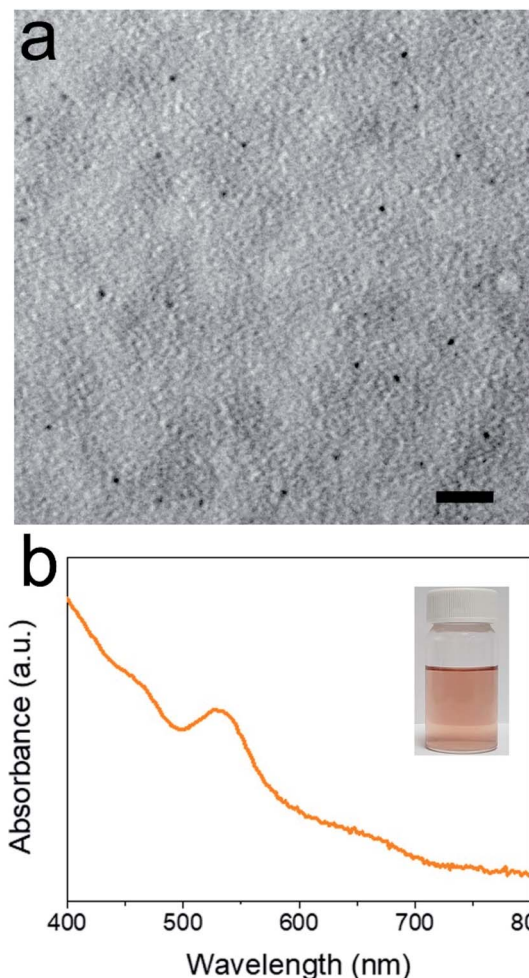
Fig. 2 Characterizations of AuNCs. (a) TEM image of AuNCs. The scale bar is 10 nm. (b) UV-visible spectrum of AuNCs. The inset is the optical picture of AuNCs.

approach. Graphene can be synthesized using colloidal solutions which can regulate the surface tension and have graphene exfoliated as well as dispersed stably.[19,32,33] Graphene is usually oxidized or functionalized first to have subsequent nanoparticle
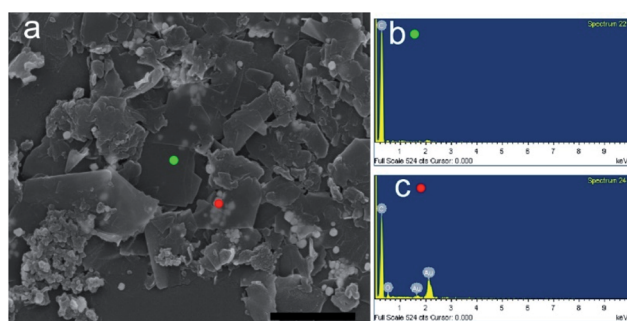

Fig. 3 Characterizations of AuNPs/graphene composite. (a) SEM image of AuNPs/graphene composite. The scale bar is 1 μm. (b) EDS analysis of green zone in (a) in which is a non-decorated graphene region. The EDS analysis only shows the carbon signal. (c) EDS analysis of red zone in (a) in which is a AuNPs-decorated region. The EDS analysis shows that there is 3.27 atomic% Au in red zone.
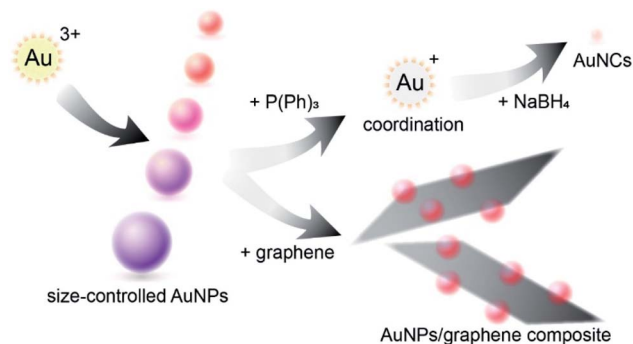

Fig. 4 A summary diagram of colloidal reduction of Au^{3+}. The synthesis result of AuNPs can be regulated using chemical kinetics and colloidal chemistry to prepare AuNPs with different sizes. In addition, with the presence of $P(Ph)_3$ ligand, the Au^+ complex would form and can be further reduced to be AuNCs. On the other hand, due to the advantage of colloidal solution, AuNPs/graphene composite can be synthesized by a simple hydrothermal approach.

decoration processes more efficient.[34] The preparations of nanoparticle/graphene composite, as a result, require additional steps and energies. With the advantage of colloidal solution, on the other hand, AuNPs can easily be decorated onto graphene by a hydrothermal approach. Fig. 3a shows a scanning electron microscopy (SEM) image of AuNPs/graphene composite. Moreover, energy-dispersive X-ray spectroscopy (EDS) demonstrates the chemical composition of the composite. Fig. 3b shows a non-decorated graphene part in which only carbon signal is detected. In Fig. 3c, on the other hand, Au signal (3.27 atomic%) is detected, indicating the successful decoration. The facile decoration may be facilitated by micelle–micelle coalescence which allows the collisions between AuNPs and graphene more effectively. Additionally, both materials possess high surface energies, so they are relatively active.[35–37] Therefore, the micelles also work as nanoreactors in which graphene can be decorated by AuNPs.

Fig. 4 shows a summary diagram of the proposed approach. Au^{3+} can be reduced to be AuNPs with controllable sizes according to the government of chemical kinetics and colloidal chemistry. To overcome the phase challenges of Au-based materials, AuNCs and AuNPs/graphene composite were synthesized as the demonstrations of the benefit of the colloidal reduction. The colloidal solution allows $P(Ph)_3$ ligand which can form Au^+ complex to disperse homogeneously and AuNCs can then be synthesized. Besides, using a simple hydrothermal approach, AuNPs can be decorated onto graphene under colloidal solution without pre-treatments of graphene by oxidation or functionalization.

Conclusions

In conclusion, utilizing chemical kinetics and colloidal chemistry, we have successfully reduced Au^{3+} to be size-controlled AuNPs, AuNCs, and AuNPs/graphene composite. Different states or morphologies of Au are expected to be used in distinctive fields, while the use of aqueous or organic phase may

be a crucial concern in some applications. The proposed colloidal reduction of Au^{3+} not only provide a throughout reduction process of Au^{3+}, but also is promising to overcome phase challenge *via* the advantage of amphiphilic colloidal solution. Hence, the study may provide some essential insights in catalysis, biomedical applications, *etc*, for AuNPs, AuNCs, and AuNPs/graphene composite are in a versatile colloidal solution rather than in traditional aqueous or organic phase. Innovated results, which can be controlled by colloidal chemistry, can thus be applied on AuNPs, AuNCs AuNPs/graphene composite prepared by colloidal reduction of Au^{3+}.

Conflicts of interest

There are no conflicts to declare.

Acknowledgements

Notes and references

1 M.-C. Daniel and D. Astruc, *Chem. Rev.*, 2004, **104**, 293–346.
2 D. Pflaesterer and A. S. K. Hashmi, *Chem. Soc. Rev.*, 2016, **45**, 1331–1367.
3 C. Wang and D. Astruc, *Chem. Soc. Rev.*, 2014, **43**, 7188–7216.
4 J. Zhao and R. Jin, *Nano Today*, 2018, **18**, 86–102.
5 R. A. Sperling, P. R. Gil, F. Zhang, M. Zanella and W. J. Parak, *Chem. Soc. Rev.*, 2008, **37**, 1896–1908.
6 B. Hvolbæk, T. V. Janssens, B. S. Clausen, H. Falsig, C. H. Christensen and J. K. Nørskov, *Nano Today*, 2007, **2**, 14–18.
7 W. Zi and F. D. Toste, *Chem. Soc. Rev.*, 2016, **45**, 4567–4589.
8 C. Wang and C. Yu, *Rev. Anal. Chem.*, 2013, **32**, 1–14.
9 M. Homberger and U. Simon, *Philos. Trans. R. Soc., A*, 2010, **368**, 1405–1453.
10 N. Elahi, M. Kamali and M. H. Baghersad, *Talanta*, 2018, **184**, 537–556.
11 M. Gao, A. Lyalin and T. Taketsugu, *J. Phys. Chem. C*, 2012, **116**, 9054–9062.
12 J. Piella, N. G. Bastús and V. Puntes, *Chem. Mater.*, 2016, **28**, 1066–1075.
13 F. Shiba, *CrystEngComm*, 2013, **15**, 8412–8415.
14 S. S. Zalesskiy, A. E. Sedykh, A. S. Kashin and V. P. Ananikov, *J. Am. Chem. Soc.*, 2013, **135**, 3550–3559.
15 A. Molter and F. Mohr, *Coord. Chem. Rev.*, 2010, **254**, 19–45.
16 Y.-M. Wang, A. D. Lackner and F. D. Toste, *Acc. Chem. Res.*, 2014, **47**, 889–901.
17 N. Khlebtsov and L. Dykman, *Chem. Soc. Rev.*, 2011, **40**, 1647–1671.
18 K. Zheng, M. I. Setyawati, D. T. Leong and J. Xie, *ACS Nano*, 2017, **11**, 6904–6910.
19 A. Ciesielski and P. Samorì, *Chem. Soc. Rev.*, 2014, **43**, 381–398.
20 M. Pileni, *J. Phys. Chem.*, 1993, **97**, 6961–6973.
21 C. Chern, *Prog. Polym. Sci.*, 2006, **31**, 443–486.
22 C. de Mello Donega, *Chem. Soc. Rev.*, 2011, **40**, 1512–1546.
23 Y. Xu, L. Chen, X. Wang, W. Yao and Q. Zhang, *Nanoscale*, 2015, **7**, 10559–10583.
24 J. Ramírez, M. Sanaú and E. Fernández, *Angew. Chem., Int. Ed.*, 2008, **47**, 5194–5197.
25 J. Wang, X. Mi, J. Wang and Y. Yang, *Green Chem.*, 2017, **19**, 634–637.
26 E. Ruckenstein and R. Nagarajan, *J. Phys. Chem.*, 1975, **79**, 2622–2626.
27 S. Förster and M. Antonietti, *Adv. Mater.*, 1998, **10**, 195–217.
28 N. T. Thanh, N. Maclean and S. Mahiddine, *Chem. Rev.*, 2014, **114**, 7610–7630.
29 D. McQueen and J. Hermans, *J. Colloid Interface Sci.*, 1972, **39**, 389–394.
30 N. A. Volkov, A. K. Shchekin, N. V. Tuzov, T. S. Lebedeva and M. A. Kazantseva, *J. Mol. Liq.*, 2017, **236**, 414–421.
31 S. Chauhan and K. Sharma, *J. Chem. Thermodyn.*, 2014, **71**, 205–211.
32 M. J. Fernández-Merino, J. Paredes, S. Villar-Rodil, L. Guardia, P. Solís-Fernández, D. Salinas-Torres, D. Cazorla-Amorós, E. Morallon, A. Martínez-Alonso and J. Tascón, *Carbon*, 2012, **50**, 3184–3194.
33 M. Lotya, P. J. King, U. Khan, S. De and J. N. Coleman, *ACS Nano*, 2010, **4**, 3155–3162.
34 P. T. Yin, S. Shah, M. Chhowalla and K.-B. Lee, *Chem. Rev.*, 2015, **115**, 2483–2531.
35 P. A. Denis and F. Iribarne, *J. Phys. Chem. C*, 2013, **117**, 19048–19055.
36 M. A. Bissett, S. Konabe, S. Okada, M. Tsuji and H. Ago, *ACS Nano*, 2013, **7**, 10335–10343.
37 T. V. Janssens, B. S. Clausen, B. Hvolbæk, H. Falsig, C. H. Christensen, T. Bligaard and J. K. Nørskov, *Top. Catal.*, 2007, **44**, 15.